

Flurbiprofen-loaded Nanoparticles Can Cross a Primary Porcine *In vitro* Blood-brain Barrier Model to Reduce Amyloid- β 42 Burden

Julia Stab^{1,2}, Iavor Zlatev³, Bastian Raudszus³, Sabrina Meister⁴, Claus U Pietrzik⁴, Klaus Langer³, Hagen von Briesen¹ and Sylvia Wagner^{1*}

¹Department Bioprocessing & Bioanalytics, Fraunhofer Institute for Biomedical Engineering, Sulzbach, Germany

²Saarland University, Saarbruecken, Germany

³Institute of Pharmaceutical Technology and Biopharmacy, University of Muenster, Germany

⁴Institute of Pathobiochemistry, University Medical Center of the Johannes Gutenberg University Mainz, Germany

*Corresponding author: Sylvia Wagner, Department Bioprocessing & Bioanalytics, Fraunhofer Institute for Biomedical Engineering, Sulzbach, Germany, Tel: +49 (0) 6897/9071-291; Fax: +49 (0) 6897/9071-490; E-mail: sylvia.wagner@ibmt.fraunhofer.de

Received date: April 07, 2016; Accessed date: April 22, 2016; Published date: April 30, 2016

Copyright: © 2016 Stab J, et al. This is an open-access article distributed under the terms of the Creative Commons Attribution License, which permits unrestricted use, distribution, and reproduction in any medium, provided the original author and source are credited.

Abstract

Elevated amyloid- β 42 (A β 42) in the brain is expected to cause Alzheimer's Disease (AD). Reducing A β 42 is therefore a cornerstone in causal drug development. Nevertheless, many promising substances failed in clinical trials, because reaching the target organ *in vivo* is difficult. The brain is protected by the Blood-Brain Barrier (BBB) that shields off most molecules to maintain the brain homeostasis. Brain-targeted nanoparticles are one successful tool to bypass this problem: by acting as Trojan horses they carry embedded drugs across the BBB for brain disorder treatment.

Here, flurbiprofen, a γ -secretase modulator, was embedded in Poly(Lactic Acid) (PLA) nanoparticles. We tested if the drug-loaded nanoparticles affected the integrity of our advanced *in vitro* BBB model in transendothelial electrical resistance measurements and permeability assays, and investigated the nanoparticle-cell interaction in flow cytometry and confocal laser scanning microscopy. Furthermore, we assessed the drug transport capacity by high-performance liquid chromatography and the biological efficacy of the embedded drug in an A β 42-detecting ELISA. We also verified the viability of the AD model cells by a cellular viability assay.

After adding flurbiprofen-loaded nanoparticles to the blood compartment of a Transwell® model, the drug was detectable in the brain compartment, where it induced an A β 42 lowering effect. Flurbiprofen from nanoparticles crossed the BBB without impairing barrier integrity, whereas the free drug was highly cytotoxic and destroyed the barrier. Ligand coupling of apolipoprotein E3 to the nanoparticles increased cellular uptake. Hence, we expect an even more pronounced A β 42 reducing effect for apolipoprotein-modified, flurbiprofen-loaded nanoparticles.

In conclusion, we enabled transport of a hardly permeable drug across an advanced *in vitro* BBB model, opening opportunities in the treatment and prevention of AD and other brain disorders. Using a primary porcine BBB model that displays excellent barrier characteristics, we show that flurbiprofen-loaded nanoparticles reduce A β 42 burden without impairing barrier function.

Keywords Blood-brain barrier; Primary *in vitro* cell culture model; Nanoparticles; Flurbiprofen; Targeted drug transport; Alzheimer's disease; Neurodegeneration; Amyloid- β 42 reduction

Flurbiprofen-loaded Poly(lactic acid) Nanoparticles; PVA: Poly(vinyl alcohol); RT: Room Temperature; TER: Transendothelial Electrical Resistance; TJ: Tight Junction; ZO-1: Zonula Occludens

Abbreviations

AD: Alzheimer's Disease; ApoE: Apolipoprotein E; APP: Amyloid Precursor Protein; A β : Amyloid β ; BBB: Blood-Brain Barrier; CHO: Chinese Hamster Ovary; Cld-3: Claudin 3; Cld-5: Claudin 5; CLSM: Confocal Laser Scanning Microscopy; CNS: Central Nervous System; DAPI: 4',6-Diamidino-2-Phenylindole; DCM: Dichloromethane; EDC: 1-Ethyl-3-(3-dimethylaminopropyl)-Carbodiimide; ELISA: Enzyme-Linked Immunosorbent Assay; FBP: Flurbiprofen; GPC: Gel Permeation Chromatography; HPLC: High Performance Liquid Chromatography; NP: Nanoparticle; NSAID: Non-Steroidal Anti-Inflammatory Drug; Occl: Occludin; Pbcc: Primary Porcine Brain Capillary Endothelial Cells; PEG: Polyethylene Glycol; PFA: Paraformaldehyde; PLA: Poly(lactic acid); PLAFBP NP:

Introduction

The Blood-Brain Barrier (BBB) is a unique structure that shields off the delicate central nervous system from the periphery in order to protect the fragile brain homeostasis. Unfortunately, the BBB also holds back most therapeutic drugs [1], such as potential anti-Alzheimer's Disease (AD) drugs. Today, more than 36 million people worldwide [2] suffer from dementia, most of the cases caused by AD. Sadly, there is neither a cure nor a prevention strategy for AD, and demographic changes heat up the situation-causing AD numbers to multiply in the next decades and resulting in enormous socio-economic burden.

Nearly 25 years ago, Hardy et al. claimed that elevated amyloid beta (A β) peptide levels in the brain cause the disease [3,4]: A β derives from consecutive cleavage of the Amyloid Precursor Protein (APP) by β - and γ -secretase, which leads to A β peptide fragments of various length. A β 42 (42 amino acids long) is highly hydrophobic and tends to form complexes—resulting in the AD's characteristic extracellular plaque formation. Modulating or blocking the activity of β - and γ -secretases to reduce A β 42 burden is therefore a cornerstone in developing causal, amyloid-based approaches in AD therapy. Other strategies comprise decreasing A β 42 aggregation or increasing A β 42 clearance to restore a non-pathogenic balance, or focus on other AD-related pathways such as Tau formation, ApoE genotypes and metabolic dysfunction (for review see [5]).

Remarkably, a cohort of people seems to be protected from AD. Retrospective studies revealed that rheumatic patients undergoing a long-term high-dose Non-Steroidal Anti-Inflammatory Drug (NSAID) therapy are less likely to develop AD than others [6,7] probably because of their pain medication: *In vitro* and *in vivo* experiments showed that NSAIDs can indeed lower A β 42 levels [8-14]. Flurbiprofen (FBP) targets γ -secretase activity and was therefore proposed as a potential anti-AD drug. Elegantly, the R-enantiomer of FBP tarenflurbil (FlurizanTM) decreases A β 42 production [15] without affecting cyclooxygenase activity, resulting in less NSAID-mediated side-effects. Nevertheless, tarenflurbil failed in a phase III clinical trial [16,17] and was therefore discontinued as an anti-AD drug, probably due to its low penetration capacity to the brain. The responsible structure—the BBB—minimizes the number of CNS drugs (e.g. for brain tumors, pain management and neurodegenerative disorders) [1]. Consequently, strategies to overcome the BBB are desperately needed, but many appear rather violent: osmotic opening of the TJs by injection of hyperosmolar mannitol solution [18] in the carotid artery, ultrasonic sound waves [19,20] to forcibly break down the barrier, or even intraventricular injection [21] or implantation of depots into the brain parenchyma [22]. Adverse side effects ranging from changes in neuropathology, brain vasculopathy and seizures [18,23-26] to intracranial infections and brain edema [27,28]. Worse, bioavailability is often very low, even for injection methods [1,29,30]. An alternative gentle, non-invasive, but effective approach for BBB crossing is nanotechnology. The first report of nanoparticle-mediated drug transport across the BBB was published in 1995 [31], and since then, countless formulations for CNS-targeting nanoparticles were developed (for reviews see [32-37]). The advantages are tempting: apart from protecting the drug from degradation in the bloodstream, nanoformulations allow high drug-loading capacities that, together with the possibility of biostructure-targeting by surface modification, may drastically reduce doses and lower adverse side-effects—making nanoparticles an excellent pharmacological tool for brain delivery (for review see [37]).

Here, we revisit flurbiprofen as a potential anti-AD drug by trying to enhance brain transport. We incorporated the drug into poly(lactic acid) nanoparticles to use them as molecular Trojan horses, masking the original physico-chemical properties of flurbiprofen that hinder transport to the brain. Our *in vitro* BBB model consists of primary porcine brain capillary endothelial cells (pBCEC) and displays excellent barrier characteristics. We convincingly demonstrated that flurbiprofen from drug-loaded poly(lactic acid) nanoparticles (PLAFBP NP) indeed crossed our advanced *in vitro* BBB without destroying barrier integrity, leading to reduced A β 42 levels in the brain-representing compartment of a Transwell[®] system and taking us one step further in anti-AD drug development. Additionally, we

surface modified nanoparticles, because BBB crossing of nanoparticles can be facilitated *in vitro* and *in vivo* by coupling of low density lipoprotein receptor family members, notably apolipoproteins [38-40] or by coating nanoparticles with surfactants that capture apolipoproteins from blood or serum [10,41], resulting in a protein corona. In pilot experiments, we confirmed here that surface modification of PLA nanoparticles with apolipoprotein E3 (ApoE) strongly increases binding to BBB model cells.

Material and Methods

Reagents and chemicals

Poly(L-lactide) (PLA, inherent viscosity ~1.0 dL/g), flurbiprofen and polyvinyl alcohol (PVA) were obtained from Sigma (Steinheim, Germany). Lumogen[®] F orange 240 was provided by BASF (Ludwigshafen, Germany). All reagents were of analytical grade.

Nanoparticle preparation & characterization

PLA nanoparticles were prepared as described earlier [10]: An organic phase (100 mg PLA and 10 mg FBP dissolved in 2 ml dichloromethane) was added to an aqueous phase (6 ml polyvinyl alcohol (2%, w/v)) and was subsequently homogenized with an Ultra Turrax[®] device (Ultra Turrax[®], IKA, Staufen, Germany) for 30 min at 24,000 rpm in an ice bath to avoid vaporization of the organic phase. Dichloromethane was removed by stirring overnight (220 rpm) under an exhaust hood. Nanoparticles were collected by centrifugation at 20,000 g for 10 min (Eppendorf, Hamburg, Germany) and redispersed in purified water. Before freeze drying, trehalose solution (6% w/v) was added 1:1 as a cryoprotective agent. Firstly, samples were frozen at -40°C for 3 hours; secondly, a vacuum of 0.05 mbar and -34°C was set for 24 hours; thirdly, temperature was raised to 20°C for 11 hours while applying a vacuum of 0.025 mbar. After drying, the vials were sealed and stored at 4°C until use. If visualization in flow cytometry and microscopy analysis was aimed for, 150 μ g of Lumogen[®] F orange 240 (BASF, Ludwigshafen, Germany) was added to the organic phase during the preparation process.

For the preparation of the apolipoprotein E3-modified nanoparticles, a PLA-nanoparticle suspension, which contained 15 mg nanoparticles, was mixed with a 5-fold molar excess—in relation to the hydroxyl groups of the PVA-of divinylsulfone (Sigma-Aldrich Chemie GmbH, Steinheim, Germany) for 5 minutes in order to introduce amine-reactive vinyl sulfone groups to the particle surface. The reaction took place in 0.1 M NaOH. Afterwards the nanoparticles were centrifuged at 10,000 g for 10 min and washed with purified water three times. The sample was centrifuged a fourth time and redispersed in 125 μ l of a solution of carboxy-(PEG)4-amine (Thermo Fisher Scientific Inc., Langensfeld, Germany) (4 mg/ml). The sample was incubated overnight at room temperature and 700 rpm. After purifying the PEGylated particles by centrifugation (10,000 g, 10 min), the pellet was redispersed in purified water. Then, the nanoparticles were treated with 80 μ l of a 1-Ethyl-3-(3-Dimethylaminopropyl)-Carbodiimide (EDC) (AppliChem, Darmstadt, Germany) solution (30 mg/ml) and a N-hydroxysulfosuccinimide (Sigma-Aldrich Chemie GmbH, Steinheim, Germany) solution (10 mg/ml), respectively and then incubated for 15 min at room temperature and 600 rpm. The suspension was buffered at a pH of 4.6 with MES during the reaction. By adding these reagents an amine-reactive sulfo-NHS ester was linked to the surface of the PEGylated nanoparticles, which can be used to connect an amine-containing molecule like a protein to the

nanoparticles covalently. In order to remove excess reagent, the activated nanoparticles were purified by centrifugation (10,000 g, 5 min) and redispersed in purified water to minimize the possibility of crosslinking between the apolipoprotein E-molecules themselves. After a second centrifugation step the nanoparticles were incubated with a solution of apolipoprotein E3 (Sigma-Aldrich Chemie GmbH, Steinheim, Germany) in phosphate buffered saline pH 7.5 (5 mg/ml) for 3 hours. Finally, the apolipoprotein E3-modified nanoparticles were centrifuged (15,000 g, 15 min) and the amount of unbound protein in the supernatant was determined in 20 μ l aliquots by Gel Permeation Chromatography (GPC) (Column: TSKgel Super SW3000, Tosoh Bioscience GmbH, Stuttgart, Germany), flow rate: 0.35 ml/min, mobile phase: phosphate buffered saline (pH 6.8; 0.1% SDS), detection at 280 nm wavelength). The prepared nanoparticles were freeze dried according to the protocol described before.

After preparation, particle diameter, Polydispersity Index (PDI) and zeta potential of PLA-FBP NP (redispersed in purified water) were analyzed with the aid of a Malvern Zetasizer Nano ZS (Malvern Instruments Ltd., Malvern, UK). For determination of flurbiprofen loading, High-Performance Liquid Chromatography (HPLC) analysis was performed: 1 ml acetonitrile was added to 1 mg nanoparticles and incubated for 5 min at room temperature. After centrifugation (20,000 g; 10 min), the 20 μ l aliquots of the supernatant were measured with a HPLC device (Column: Gemini NX 250 \times 4.6 mm, 5 μ m particle, C18 column, Phenomenex, Aschaffenburg, Germany). The flow rate was 1 ml/min and the mobile phase consisted of acetonitrile and 0.1% (v/v) trifluoroacetic acid (57.5: 42.5, v/v), detection was performed at 245 nm wavelength.

Lyophilized nanoparticles were freshly reconstituted in cell culture medium (40 mg/ml) and vortexed prior to experiments.

Cell culture

Primary porcine Brain Capillary Endothelial Cells (pBCEC) were isolated as described earlier [39,42]. In brief, fresh porcine skulls from *Sus scrofa domestica* (domestic pig) were kindly provided by the local slaughterhouse in Zweibrücken, Germany. Animals were killed in accordance to Council Directive 93/119/EC of the European Commission on the protection of animals at the time of slaughter or killing, dated December 22nd, 1993. The skulls were opened to access the brains which were freed from meninges and large blood vessels. After roughly separating white from gray matter, the gray matter was minced and sequentially treated with digestion enzymes, density gradient centrifugation, filtration and erythrocyte lysing as described earlier [39,42]. Purified pBCEC were seeded on collagen IV-coated Transwell[®] cell culture inserts with a polycarbonate membrane of 3 μ m pore size (12-well format) at 37°C and 5% CO₂ in a density of 3.6 \times 10⁵ cells/cm² in medium 199 supplemented with 10% newborn calf serum, 0.7 mM L-glutamine, 1% penicillin/streptomycin, and 1% gentamicin. Medium was exchanged to remove debris from attached cells after on 1 h in culture. The next day, medium was changed to DMEM/F12 with 5% fetal calf serum, 0.75% L-glutamine, 1% penicillin/streptomycin, 1% gentamicin, and 550 nM hydrocortisone. Further experiments were performed after 4-5 days in culture when TER was >300 Ω ·cm² and still rising (monitored by continuous Transendothelial Electrical Resistance (TER) measurement in a cellZscope[®] device).

APP751 overexpressing CHO cells (7WD10) were cultured in DMEM high glucose medium containing 10% fetal calf serum (Sigma Aldrich, Steinheim, Germany), 1 mM sodium pyruvate, 1% penicillin/streptomycin and 400 μ g/ml geneticin (all Gibco[®], Darmstadt,

Germany). 7WD10 were seeded in a density of 3 \times 10⁴ cells/cm² three hours before applying medium from the basolateral compartment of pBCEC (after drug transport experiments) for 72 h.

Antibody staining

For the characterization of the BBB model, cells were stained with various antibodies against tight junction proteins (Cld 3, Cld 5, ZO 1, Occl). Cells were fixed with 1% paraformaldehyde or acetone for 5 to 10 minutes and blocked by 5% Fetal Calf Serum (FCS) or Bovine Serum Albumin (BSA) for 20 minutes. The primary antibody was diluted in PBS and incubated at room temperature for 1 hour or at 4°C over night. Cells were washed twice with PBS before applying the secondary antibody for 1 hour. After washing with PBS, cell culture slides were allowed to dry for up to 1 hour. Then, VECTASHIELD Hard Set[™] mounting medium (with DAPI) (Vector Laboratories, Burlingame, USA) and cover glasses were added. After at least 2 hours in a refrigerator, samples were analyzed with a LSM 510 confocal microscope (Zeiss, Jena, Germany).

Measurement of the transendothelial electrical resistance of endothelial cells

With the aid of a cellZscope[®] device (nanoAnalytics, Münster, Germany), we non-invasively measured cell membrane Capacitance (Ccl) and Transendothelial Electrical Resistance (TER) by impedance spectroscopy as described earlier [42]: pBCEC seeded on Transwell[®] membranes were placed into the cellZscope[®] device, which was put into an incubator (37°C, 5% CO₂) and connected to the external controller and a computer.

Permeability of radiolabelled model substances

The quality of *in vitro* BBB model systems can also be assessed by the permeability of different marker substances. For this purpose, pBCEC were isolated and prepared as described. Permeability experiments were performed when TER was still rising (assessed with the aid of a cellZscope[®] device) at day 5 post seeding. As a paracellular marker ¹⁴C inulin (PerkinElmer, Boston, MA, USA) was chosen: inulin is not able to cross the BBB *in vivo* and therefore its low permeability represents a good indicator for intact barrier integrity. To verify physiological conditions, a transcellular marker was also applied: ¹⁴C diazepam (Hartmann Analytic GmbH, Braunschweig, Germany) (also known as Valium[®]) is a brain acting drug and diffuses through endothelial cell *in vivo*.

For barrier characterization experiments, 0.35 μ Ci/Transwell[®] of ¹⁴C inulin or ¹⁴C Diazepam (DZP) were added to the apical compartment. After 2 hours incubation, medium from the apical and basolateral Transwell[®] compartment was transferred to a plastic vial containing 6 ml scintillation fluid (Ultima Gold, PerkinElmer, Boston, MA, USA) and placed into a Liquid Scintillation Counter (LSC) (Tri-Carb 2910TR, PerkinElmer, Boston, MA, USA). The Decay Per Minute (dpm) and Counts Per Minute (cpm) data were calculated by the QuantaSmart software (PerkinElmer, Boston, MA, USA) with program settings for a single dpm assay and a measured energy level from 0 keV to 156 keV.

In order to further verify physiological conditions, the BBB model was opened by adding 80 μ l hyperosmotic 1.1 M mannitol solution (MANNIT 20, Serag-Wiessner KG, Naila, Germany) to the apical compartment.

To investigate if the nanoparticles influence the barrier integrity, 0.35 μ Ci of 14 C inulin was added to each Transwell[®] after nanoparticles and controls were applied. Again, after 2 hours incubation the medium from each compartment was collected and transferred to scintillation fluid for analysis with a liquid scintillation counter.

Cellular binding and uptake of nanoparticles

Primary cells were seeded on multi-well culture plates, previously coated with human collagen IV (131 μ g/cm²). Samples and controls were incubated for 4 hours at 37°C: nanoparticulate formulations were added in a final concentration of 105.3 μ g/cm² growth surface, fluorescence-labeled ApoE3 (Sigma-Aldrich, Steinheim, Germany, labeled with PromoFluor-633 Labeling Kit, PromoCell GmbH, Heidelberg, Germany) was added in a concentration of 1.053 μ g/cm² growth surface to simulate the approximate concentration of ApoE3 on ApoE3-modified nanoparticles (10 μ g ApoE3/1 mg nanoparticle). After incubation, the cells were washed twice with PBS, detached from the growth surface and transferred into FACS tubes. Cells were again washed two times with PBS and subsequently fixed with FACS-Fix solution consisting of 10 g/l PFA (Sigma-Aldrich, Steinheim, Germany) and 8.5 g/l NaCl (Sigma-Aldrich, Steinheim, Germany) in PBS (Gibco[®], Darmstadt, Germany). For flow cytometry analysis, at least 10,000 cells per sample were counted and evaluated with the aid of *CellQuest Pro* software (untreated control cells were used for population gating). Lumogen[®] F Orange 240 labeled PLA nanoparticles were detected in fluorescence channel FL-1 (Ex 488/Em 530), PromoFluor-633 labeled ApoE3 was detected in FL-4 (Ex 633/Em 661).

Cellular uptake of nanoparticles can be monitored by Confocal Laser Scanning Microscopy (CLSM). For this purpose, pBCEC were seeded on human collagen IV-coated glass cover slides (Becton Dickinson, Heidelberg, Germany) and incubated with 105.3 μ g/cm² of different Nano particular formulations for 37°C for 4 or 24 hours. After washing with PBS, cells were incubated with CellTracker[™] Blue CMAC, according to the manufacturer's instructions to stain the cytosol. Then, samples were fixed with 1% paraformaldehyde (Sigma-Aldrich, Steinheim, Germany) for 10 minutes at room temperature, dried and embedded in VECTASHIELD Hard Set[™] mounting medium (Vector Laboratories, Burlingame, USA). Microscopy analysis was performed with a TCS SP8 confocal microscope (Leica Microsystems, Heidelberg, Germany). PLA nanoparticles were labeled with Lumogen[®] F Orange 240 for detection at 524/539 nm wavelength.

Nanoparticle transport experiments

pBCEC were isolated and seeded on Transwell[®] inserts in a cellZscope[®] device as described. Four days later, pBCEC were incubated with PLAFBP NP or FBP for 4 hours, afterwards medium from apical and basolateral compartment was collected for analysis or further experiments.

Quantification of drug transport: For quantitative detection of flurbiprofen, we analyzed the samples with High Performance Liquid Chromatography (HPLC) for flurbiprofen content. 400 μ l of apical or basolateral sample were mixed with 800 μ l acetonitrile to precipitate proteins and centrifuged (30,000 g, 30 min). Transwell[®] membranes were dissolved by adding 1 ml DMSO and centrifuged (10,000 g, 10 min) to remove polycarbonate residues. Supernatants were transferred to fresh vials and were analyzed by HPLC analysis (Table 1).

Equipment	Agilent 1200 or 1260 Infinitely Series HPLC device
Column	Gemini [®] -NX C18 or Poroshell 120EC-C18
Mobile phase	57.5% acetonitrile: 42.5% trifluoroacetic acid (0.1% in water)
Flow rate	1 or 0.5 ml/min
Column compartment temperature	30 or 40°C
Detection	Diode array detector, 245 or 247 nm
Injection volume	20 or 10 μ l
Runtime	8 min

Table 1: Conditions used for quantification of drug transport.

Measurement of A β 42 species by ELISA: After pBCEC were incubated with PLA-FBP NP or FBP for 4 h, medium from the basolateral compartment was transferred to 7WD10 cells for further 72 h to investigate the influence on A β 42 burden. Levels of A β 42 (and not A β 40/43) can be selectively and quantitatively detected with a commercially available ELISA kit (Invitrogen, Karlsruhe, Germany) that was performed according to the manufacturer's instructions: in the first step, standards of known A β 42 concentration (15.63–1,000 pg/ml), samples and controls were co-incubated with an antibody specific for the Cterminus of the 1-42 A β sequence in a microtiter plate coated with an antibody specific for the Nterminus of the A β peptide. As recommended, the protease inhibitor cocktail 4 (2-aminoethyl)benzenesulfonyl fluoride hydrochloride (AEBSF) (Sigma Aldrich, Steinheim, Germany) was added in a final concentration of 1 mM. Bound antibody was detected by adding a Horseradish Peroxidase (HRP)-labeled antibody that recognizes the species origin of the anti A β 42 peptide antibody. Next, the HRP substrate (stabilized chromogen) was added and converted to a bluish color by HRP (directly proportional to the amount of A β 42). The reaction was stopped by a stop solution that changes color from blue to yellow and enabled detection at 450 nm with a common plate reader (TECAN infinite 200, Tecan Group Ltd., Maennedorf, Switzerland). Negative controls included chromogen blanks. All samples and standards were performed at least in duplex per assay. Untreated 7WD10 cell controls were set as 100% A β 42 level.

Cellular viability of the Alzheimer's disease model cells

In order to exclude cytotoxic effects that could falsify the outcome of A β 42 reduction, we also performed the cellular viability assay after transport experiments across the pBCEC *in vitro* BBB model. Samples and controls were added to Transwell[®] inserts seeded with pBCEC as described earlier. After 4 hours of incubation, the basolateral medium was transferred to 7WD10 cells and after 72 hours, the supernatant was analyzed for A β 42 species and flurbiprofen content. The 7WD10 cells were washed with PBS and provided with fresh medium containing 1% alamarBlue[®] overnight in an incubator and analyzed for fluorescence intensity (excitation 560 nm, emission 610 nm).

Results and Discussion

Nanoparticle characteristics

Poly(lactic acid) (PLA) is a common basis material for nanoparticle preparation: it is biocompatible and approved in a vast number of applications, ranging from wrapping and catering material, agricultural use to medical technology, e.g. surgical implants. The main advantage in this field is the human body's capability to degrade PLA, which was first described nearly 50 years ago [43].

Here, PLA nanoparticles were prepared by an emulsion-diffusion method. Incorporation of an optional fluorescent dye (Lumogen[®] F Orange 240) allowed visualization. During the preparation process flurbiprofen was added and incorporated into the nanoparticles (PLAFBP NP): the mean loading leveled off at $52.3 \pm 11.3 \mu\text{g}$ flurbiprofen per 1 mg nanoparticle. The mean nanoparticle diameter was $239.9 \pm 11.2 \text{ nm}$, the poly dispersity index 0.070 ± 0.026 indicates a monodisperse (homogeneous) particle population. Under the described preparation conditions about $31 \mu\text{g}$ apolipoprotein E3 (ApoE) per 1 mg nanoparticle was bound to the drug carrier system. However, the ApoE binding could be differentiated in a covalently attached portion of the protein ($15 \mu\text{g}/\text{mg}$) and an adsorptively attached part ApoE ($16 \mu\text{g}/\text{mg}$). The nanoparticles were characterized by a zeta potential of $-42.5 \pm 9.6 \text{ mV}$, indicating a sufficient electrostatic stabilization of the colloidal structure.

A primary porcine *in vitro* blood-brain barrier model for drug transport studies

We performed various quality tests to verify appropriate barrier characteristics of our porcine *in vitro* Blood-Brain Barrier (BBB) model: 4 days after preparation and seeding, we checked for Tight Junction (TJ) protein expression, Transendothelial Electrical Resistance (TER) development and ^{14}C labeled marker permeability.

TJ proteins are the cornerstones of the BBB's integrity, sealing the gaps between the endothelial cells and shutting the paracellular route for substances. Accurate TJ protein expression is therefore essential for a BBB model. Antibody staining revealed that Porcine Brain Capillary Endothelial Cells (pBCEC) express the key TJ proteins claudin 3 (Cld-3), claudin 5 (Cld-5), occludin (Occ) and zonula occludens (ZO-1) (Figure 1).

Another important parameter of *in vitro* BBB models is the TER of the cells that can be measured by impedance spectroscopy using a cellZscope[®] device. In our studies, we included pBCEC grown on $3 \mu\text{m}$ pore-sized Transwell[®] membranes that developed TER values $>300 \Omega\cdot\text{cm}^2$ after 4 to 5 days in culture (Figure 2A). To check if the achieved TER values are sufficient for appropriate barrier integrity, we performed permeability assays with radiolabelled marker substances: Inulin is neither actively transported across the BBB, nor diffuses to the brain *in vivo*. Our pBCEC Transwell[®] model is impermeable for inulin ($<0.2\%$ ^{14}C inulin permeability), indicating a strong barrier function comparable to the *in vivo* situation (Figure 2B).

Application of 20% mannitol solution to pBCEC increased ^{14}C inulin permeability up to 3.5%, confirming the physiological properties in terms of osmotic opening. Diazepam, a psychiatric, highly lipophilic drug, crosses the BBB *in vivo* and therefore represents a transcellular marker to investigate *in vitro* BBB quality: In our pBCEC model, 6.1% of ^{14}C diazepam crossed the Transwell[®], and as expected, permeability for ^{14}C diazepam increased when co-applying

mannitol to force the barrier to open. Collagen IV-coated Transwell[®] inserts without cells were used to assess the amount of ^{14}C labeled substances held back by the polycarbonate membranes alone.

Influence on pBCEC cellular viability and barrier integrity

For drug transport experiments, it is essential that a BBB model displays appropriate barrier characteristics in order to exclude false positive results. With the aid of a cellZscope[®] device, we assessed if the nanoparticles influence TER of pBCEC and showed that PLAFBP NP barely affected long-term TER development. After a concentration-dependent drop in TER, pBCEC quickly recovered to TER values comparable to control cells when PLAFBP NP were applied (Figures 3A and 3B).

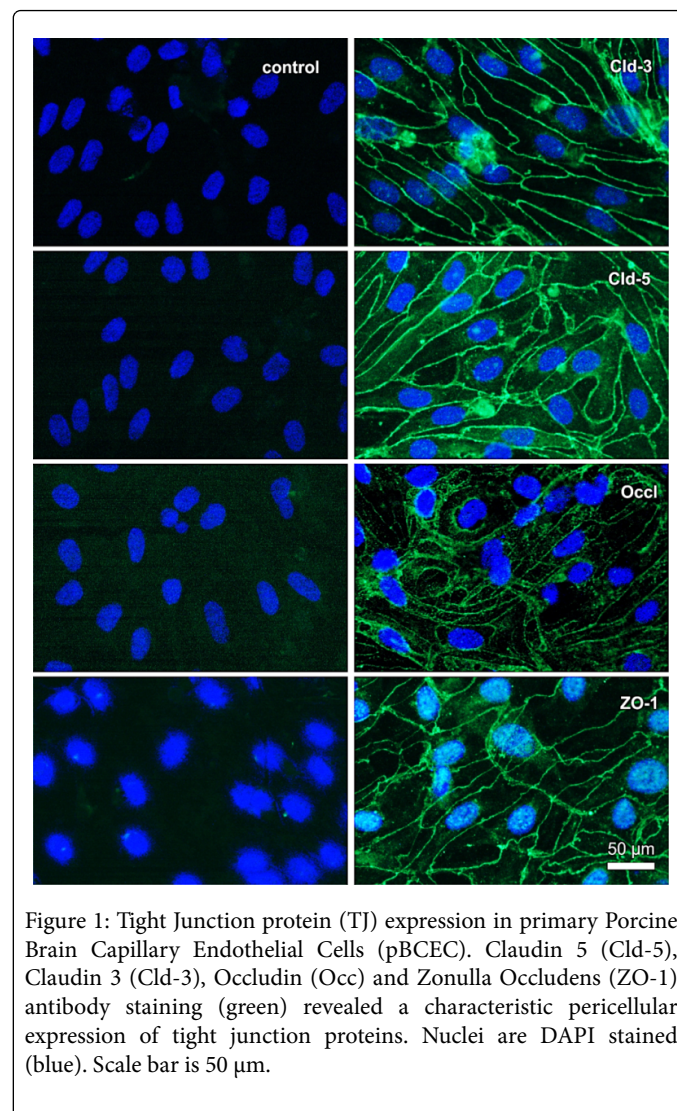


Figure 1: Tight Junction protein (TJ) expression in primary Porcine Brain Capillary Endothelial Cells (pBCEC). Claudin 5 (Cld-5), Claudin 3 (Cld-3), Occludin (Occ) and Zonula Occludens (ZO-1) antibody staining (green) revealed a characteristic pericellular expression of tight junction proteins. Nuclei are DAPI stained (blue). Scale bar is $50 \mu\text{m}$.

In contrast, addition of FBP resulted in a massive TER impairment that did not recover in the following hours. Similar results were obtained in permeability studies with the radioactive-labeled paracellular marker ^{14}C inulin: PLAFBP NP did not alter ^{14}C inulin permeability, ruling out that the drop in TER after PLAFBP NP application might symptomize a short-term reversible barrier disruption (Figure 3C).

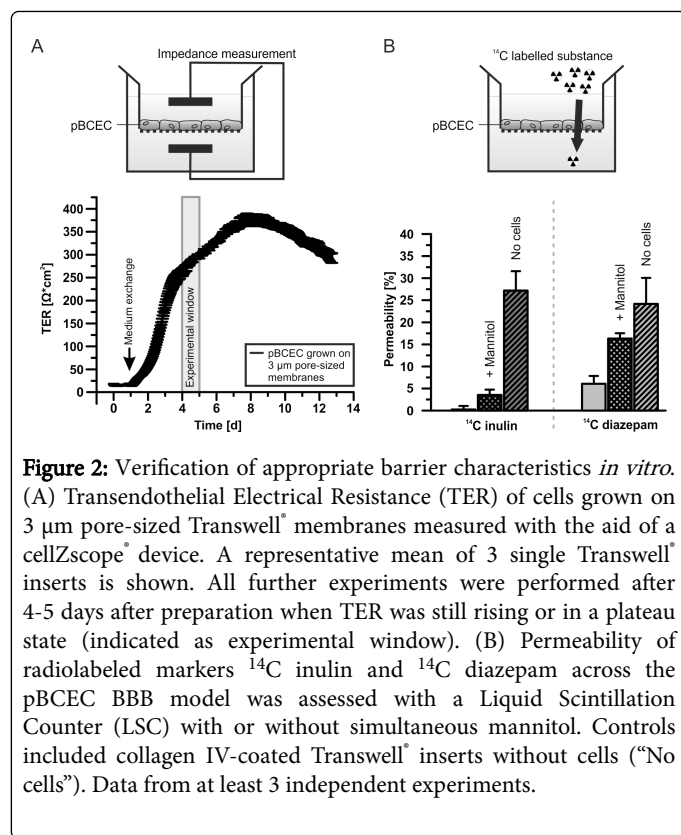


Figure 2: Verification of appropriate barrier characteristics *in vitro*. (A) Transendothelial Electrical Resistance (TER) of cells grown on 3 μm pore-sized Transwell[®] membranes measured with the aid of a cellZscope[®] device. A representative mean of 3 single Transwell[®] inserts is shown. All further experiments were performed after 4-5 days after preparation when TER was still rising or in a plateau state (indicated as experimental window). (B) Permeability of radiolabeled markers ^{14}C inulin and ^{14}C diazepam across the pBCEC BBB model was assessed with a Liquid Scintillation Counter (LSC) with or without simultaneous mannitol. Controls included collagen IV-coated Transwell[®] inserts without cells ("No cells"). Data from at least 3 independent experiments.

However, even low concentrations of FBP increased ^{14}C inulin permeability to a value comparable to simultaneous mannitol-forced opening of the *in vitro* model; higher concentrations completely abolished the barrier function (compare to Figure 2B). Finally, we investigated if PLAFBP NP influenced cellular viability in alamarBlue[®] assays. pBCEC that generally react very sensitive to external stimuli, tolerated PLAFBP NP even in high concentrations whereas free FBP decreased cellular viability (Figure 3D).

Cellular binding and uptake of flurbiprofen-loaded poly(lactic acid) nanoparticles

In flow cytometry experiments, we observed that the fluorescent, flurbiprofen-loaded PLA nanoparticles (PLAFBPLum NP) bound to nearly 100% of the BBB model cells (Figure 4A). Furthermore, we investigated the nanoparticle uptake potential of pBCECs with the aid of a confocal laser scanning microscope. Whereas untreated control samples lacked cell-associated nanoparticle signals (Figure 4B), nanoparticle-treated cells displayed a correlation between the cytosolic staining and the signal for PLAFBPLum NP (Figure 4C, 4D). It appeared that the nuclei of the cells were not infiltrated with the fluorescent labeling molecules of the nanoparticles.

Nanoparticle-mediated drug transport

We incubated increasing amounts of drug-loaded nanoparticles (PLAFBP NP) in the apical ("blood") compartment and checked for flurbiprofen content in the basolateral ("brain") compartment by High Performance Liquid Chromatography (HPLC) analysis after 4 hours (Figure 5A). We observed flurbiprofen from PLAFBP NP crossed the pBCEC barrier in a concentration dependent manner (Figure 5B). Expressed in percentage, we found that more than 40% of the apically

applied drug was detectable in the basolateral compartment (Figure 5C). We retrieved about 90% of the drug from PLAFBP NP when we also analyzed the apical compartment and dissolved the Transwell[®] membrane seeded with pBCEC. About 6% of the detected drug is located in the Transwell[®] membrane indicating that a proportion of PLAFBP NP was endocytosed, but unable to release the incorporated drug, or was not transcytosed by pBCEC during incubation time (Figure 5D).

In sum, the HPLC data shows that flurbiprofen-loaded nanoparticles are indeed capable of transporting the drug across an *in vitro* BBB model. This result is particularly interesting, because *in vivo*, flurbiprofen tightly binds to plasma proteins [44]. Therefore, availability of flurbiprofen in the brain is very restricted, potentially prohibiting a neuroprotective effect regarding Alzheimer's disease pathology. In fact, only >5% of applied acidic NSAIDs (ibuprofen, flurbiprofen, ketoprofen, naproxen) reach the brain or the Cerebrospinal Fluid (CSF) [15,44-47]. Nanoparticles are expected to prevent a plasma protein binding effect of flurbiprofen, thereby increasing CNS transport.

A β 42 reduction by flurbiprofen-loaded poly(lactic acid) nanoparticles

In order to assess if the incorporated flurbiprofen from PLAFBP NP can still reduce A β 42 levels *in vitro*, we transferred media from the basolateral compartments to A β 42 overexpressing 7WD10 cells, representing an Alzheimer's disease model (Figure 6A). We found that the transported flurbiprofen from PLAFBP NP reduced A β 42 levels to nearly 60% of the control levels (Figure 6B).

Importantly, PLAFBP NP hardly influence neither TER nor barrier integrity and are attractive for their very low cytotoxic potential in contrast to the free drug (Figure 3) confirming that the flurbiprofen from nanoparticles crossed an intact barrier.

Cellular viability of the Alzheimer's disease model cells 7WD10

In order to exclude that the drug-loaded nanoparticles may decrease cellular viability of the Alzheimer's disease model (leading to false positive results for A β 42 reduction), we performed cytotoxicity assays after transport studies. PLAFBP NP were incubated at the apical site of the *in vitro* pBCEC BBB model for 4 hours, then the medium from the basolateral compartment was transferred to 7WD10 cells for 72 hours (Figure 7A). All treated 7WD10 cells displayed viability values near 100% compared to untreated control cells (Figure 7B), ruling out that an A β 42 decreasing effect was due to cytotoxic effects.

Surface modification of poly(lactic acid) nanoparticles

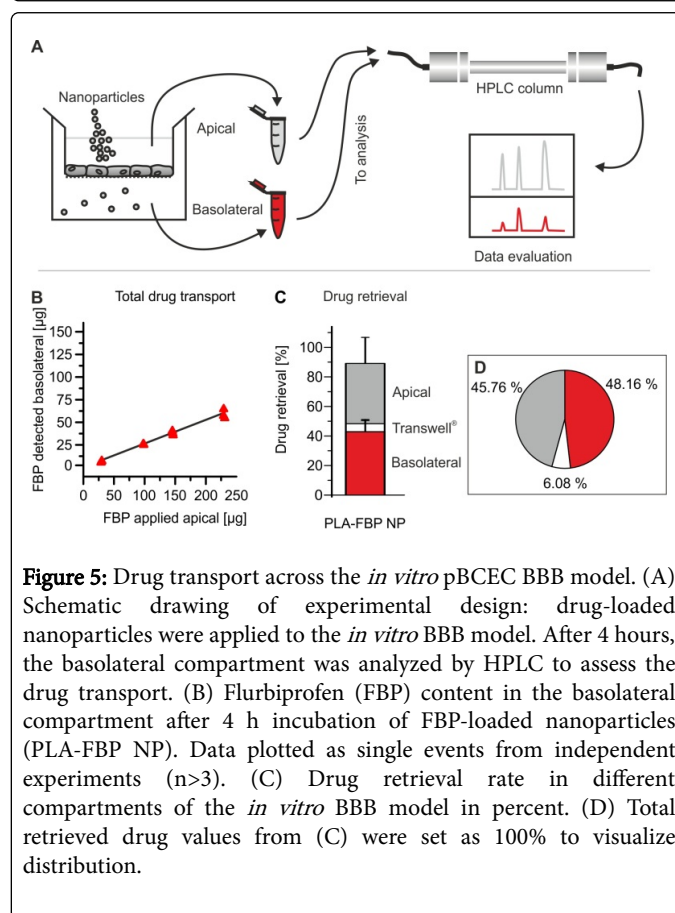
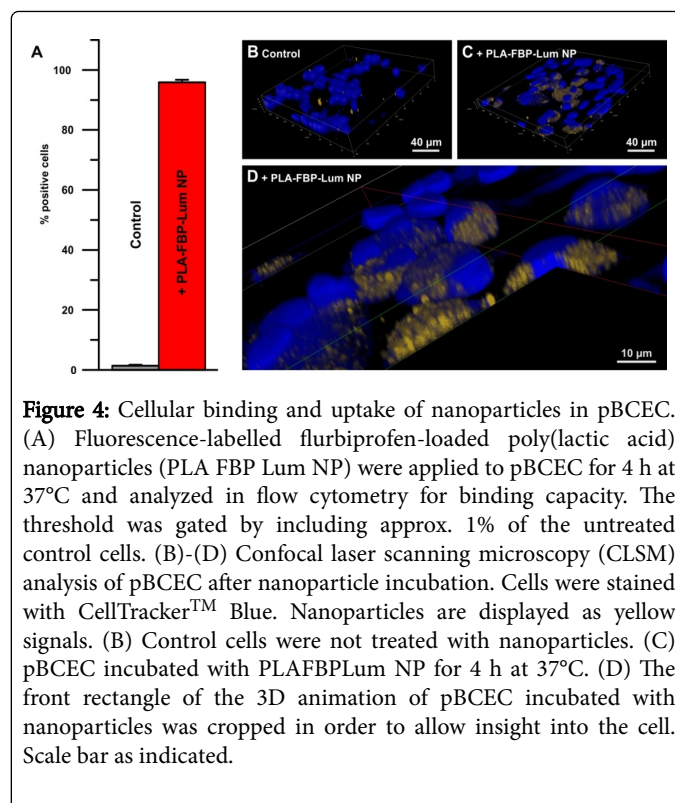
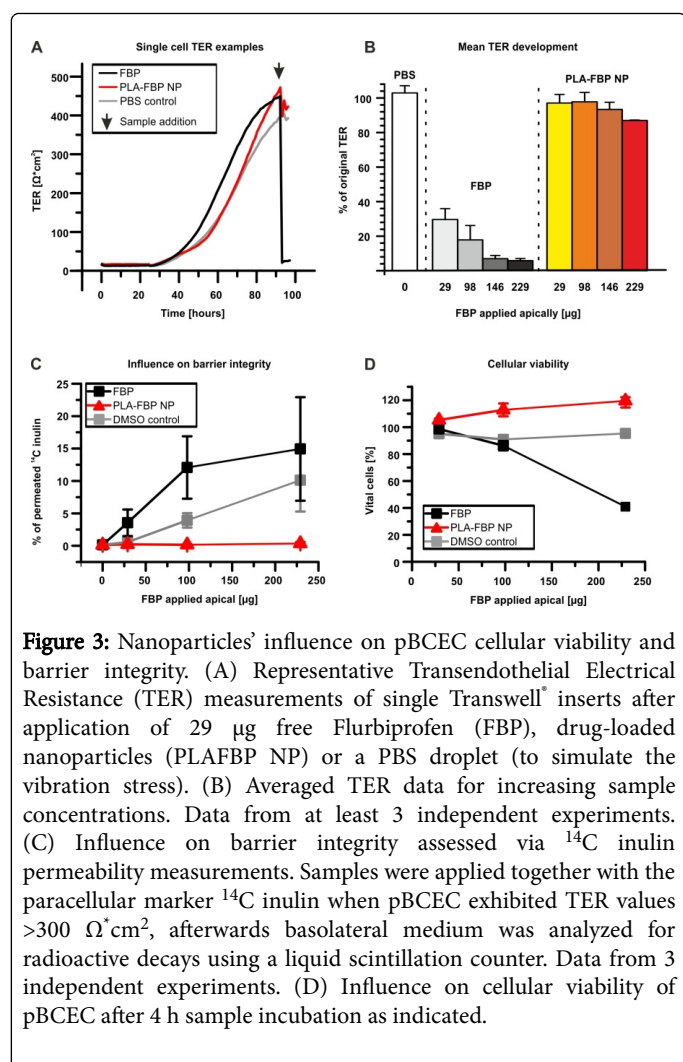
The previously described experiments in this study were performed by using unmodified, drug-loaded nanoparticles. In an earlier publication, we discussed that these nanoparticles form a protein corona after human plasma incubation. This corona contains apolipoproteins that can increase BBB translocation [10]. We and others [38,39,41] showed that coupling of ligands to the nanoparticle surface can be relevant for BBB uptake. Zensi et al., for example, used ApoE-modification of human serum albumin nanoparticles to successfully achieve brain uptake and delivery to neurons in rodents after injection into the jugular vein [38]. The underlying uptake mechanism of ApoE-modified nanoparticles is an active transcytosis

process, initiated by the binding of apolipoproteins to members of the low density lipoprotein receptor family (especially to the low density Lipoprotein Receptor Related Protein 1 (LRP1)) [39]. Here, we PEGylated the nanoparticles' surface to allow coupling of the ligand ApoE3 and control proteins. Flow cytometry experiments revealed that incubating endothelial cells with ApoE3-modified poly(lactic acid) nanoparticles (PLA-PEG-ApoE NP) drastically enlarged binding capacity, compared to unmodified nanoparticles (PLA NP) (Figure 8).

When the preparation procedure of the PLA-PEG-ApoE NP was slightly changed (and lacked NaOH in the buffer composition in order to diminish ApoE3 binding reactions), binding capacity dropped again and compared to unmodified PLA NP. Coupling of the random protein ovalbumin showed equal binding of unmodified PLA NP to pBCEC. From this promising data, we conclude that ApoE-modification of PLA nanoparticles could also increase the amount of transported flurbiprofen across our BBB model.

Conclusion

Flurbiprofen was proposed as a promising anti-Alzheimer's disease drug candidate decades ago, since it lowers neurotoxic A β 2 burden *in vitro* and *in vivo*. Nevertheless, the drug only poorly crosses the BBB, therefore restricting the maximal dose achievable in the brain.



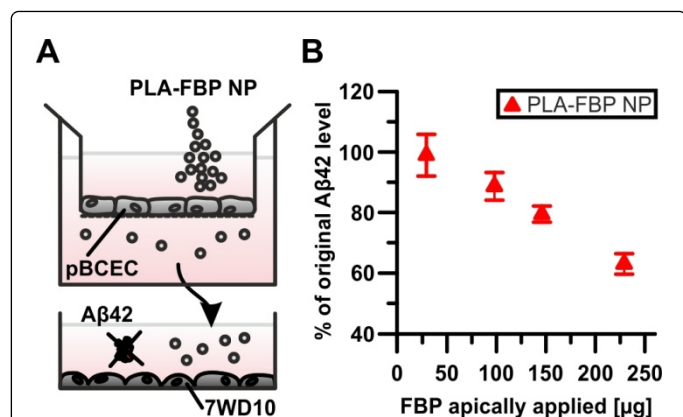


Figure 6: A β 42-lowering capacity of nanoparticles after *in vitro* BBB crossing. (A) Schematic drawing of experimental design: pBCEC were isolated and cultivated as described earlier. When Transendothelial Electrical Resistance (TER) was adequate, we added drug-loaded nanoparticles (PLA-FBP NP) for 4 hours. Then, the apical compartment and pBCEC were discarded and basolateral medium was transferred to culture plates seeded with A β 42 producing 7WD10 cells for 72 hours. (B) Analysis of 7WD10 supernatants by a human A β 42 recognizing ELISA assay. Data from at least 3 independent experiments.

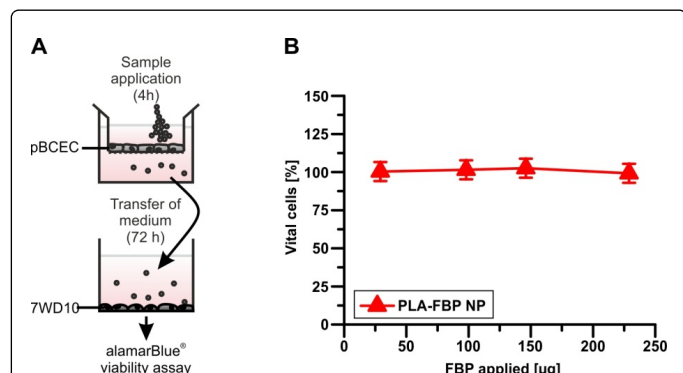


Figure 7: Influence of free drug or nanoparticles on the AD model cells' viability. (A) Schematic drawing of experimental design: pBCEC were incubated with increasing concentrations of PLAFBP NP for 4 h. Then, medium of the basolateral compartment was transferred to the Alzheimer's disease model cells 7WD10 for 72 hours before performing an alamarBlue® cellular viability assay. (B) Cellular viability of pBCEC after PLAFBP NP incubation. Untreated control cells were set as 100% vital. Data from at least 3 independent experiments.

In this study, we loaded (poly lactic)acid nanoparticles with flurbiprofen (PLAFBP NP) and verified that the drug crossed our pBCEC BBB model without impairing barrier integrity, and was able to lower A β 42 levels in a subsequent cellular Alzheimer's disease model. Controls of DMSO-dissolved Flurbiprofen (FBP) also decreased A β 42 burden, but completely impaired barrier function, making PLAFBP NP an advantageous tool for flurbiprofen delivery to the brain.

Coupling of apolipoprotein E3 to PLA nanoparticles increased binding capacity to BBB model cells in pilot experiments, suggesting that nanoparticle-mediated drug transport can also be enlarged by surface modification. The underlying endo- and transcytosis processes are mediated by binding of the nanoparticles to receptors of the Low Density Lipoprotein (LDL) receptor family (for review see [37]) expressed at the BBB. Here, binding of PLA nanoparticles to the specific receptors was either achieved by direct ApoE-coupling to the nanoparticles or by adsorption of apolipoproteins from the serum in the cell culture medium to PLA nanoparticles as reported in [10].

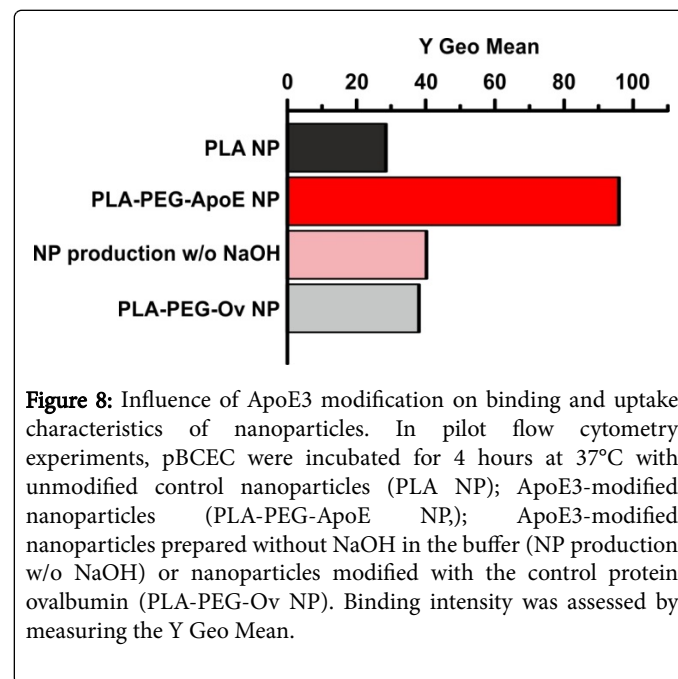


Figure 8: Influence of ApoE3 modification on binding and uptake characteristics of nanoparticles. In pilot flow cytometry experiments, pBCEC were incubated for 4 hours at 37°C with unmodified control nanoparticles (PLA NP); ApoE3-modified nanoparticles (PLA-PEG-ApoE NP); ApoE3-modified nanoparticles prepared without NaOH in the buffer (NP production w/o NaOH) or nanoparticles modified with the control protein ovalbumin (PLA-PEG-Ov NP). Binding intensity was assessed by measuring the Y Geo Mean.

All in all, this study underpins the idea of nanoparticles acting as molecular "Trojan horses" to guide drugs across the BBB—verifying that nanoparticles represent an elegant tool for overcoming the BBB with minimal invasive damage in order to transport drug to the CNS.

Conflicts of Interest

The authors declare that neither competing financial interests nor non-financial conflicts of interest exist for any of the authors.

Authors' Contributions

JS and SW designed the experimental setup. JS performed and SM contributed to the experiments. SW supervised the experiments. IZ and BR prepared the nanoparticles used in this study. JS drafted the manuscript. IZ, BR, SM, KL, CUP, HVB and SW helped to draft and/or revised the manuscript. All authors read and approved of the final manuscript.

Acknowledgement

We thank Sascha Wien for excellent technical support. This work was financially supported by the BMBF (01EW1009; 01EW1010).

References

- Pardridge WM (2005) The blood-brain barrier: bottleneck in brain drug development. *NeuroRx* 2: 3-14.
- Querfurth HW, LaFerla FM (2010) Alzheimer's disease. *N Engl J Med* 362: 329-344.
- Hardy J, Allsop D (1991) Amyloid deposition as the central event in the aetiology of Alzheimer's disease. *Trends Pharmacol Sci* 12: 383-388.
- Hardy J, Higgins G (1992) Alzheimer's disease: the amyloid cascade hypothesis. *Science* 256: 184-185.
- Citron M (2010) Alzheimer's disease: strategies for disease modification. *Nat Rev Drug Discov* 9: 387-398.
- Launer L (2003) Nonsteroidal anti-inflammatory drug use and the risk for Alzheimer's disease: dissecting the epidemiological evidence. *Drugs* 63: 731-739.
- Mayeux R (2008) Alzheimer's disease: epidemiology. *Handbook of Clinical Neurology* 89: 195-205.
- Combs CK, Johnson DE, Karlo JC, Cannady SB, Landreth GE (2000) Inflammatory mechanisms in Alzheimer's disease: inhibition of beta-amyloid-stimulated proinflammatory responses and neurotoxicity by PPAR γ agonists. *J Neurosci* 20: 558-567.
- Heneka MT, Landreth GE, Feinstein DL (2001) Role for peroxisome proliferator-activated receptor- γ in Alzheimer's disease. *Ann Neurol* 49: 276.
- Meister S, Zlatev I, Stab J, Docter D, Baches S, et al. (2013) Nanoparticulate flurbiprofen reduces amyloid- β 42 generation in an *in vitro* blood-brain barrier model. *Alzheimers Res Ther* 5: 51.
- Cole GM, Morihara T, Lim GP, Yang F, Begum A, et al. (2004) NSAID and antioxidant prevention of Alzheimer's disease: lessons from *in vitro* and animal models. *Ann N Y Acad Sci* 1035: 68-84.
- Gasparini L, Ongini E, Wenk G (2004) Non-steroidal anti-inflammatory drugs (NSAIDs) in Alzheimer's disease: old and new mechanisms of action. *J Neurochem* 91: 521-36.
- Leuchtenberger S, Beher D, Weggen S (2006) Selective modulation of Abeta42 production in Alzheimer's disease: non-steroidal anti-inflammatory drugs and beyond. *Curr Pharm Des* 12: 4337-4355.
- Beher D, Clarke EE, Wrigley JD, Martin ACL, Nadin A, et al. (2004) Selected non-steroidal anti-inflammatory drugs and their derivatives target gamma-secretase at a novel site. Evidence for an allosteric mechanism. *J Biol Chem* 279: 43419-43426.
- Eriksen JL, Sagi SA, Smith TE, Weggen S, Das P, et al. (2003) NSAIDs and enantiomers of flurbiprofen target gamma-secretase and lower Abeta 42 *in vivo*. *J Clin Invest* 112: 440-449.
- (2008). Myriad Genetics Reports Results of U.S. Phase 3 Trial of FlurizanTM in Alzheimer's Disease.
- Green RC, Schneider LS, Amato DA, Beelen AP, Wilcock G, et al. (2009) Effect of tarenflurbil on cognitive decline and activities of daily living in patients with mild Alzheimer disease: a randomized controlled trial. *JAMA* 302: 2557-2564.
- Neuwelt EA, Rapoport SI (1984) Modification of the blood-brain barrier in the chemotherapy of malignant brain tumors. *Fed Proc* 43: 214-219.
- Konofagou EE, Tung Y-S, Choi J, Deffieux T, Baseri B, et al. (2012) Ultrasound-induced blood-brain barrier opening. *Curr Pharm Biotechnol* 13: 1332-1345.
- Alonso A (2015) Ultrasound-induced blood-brain barrier opening for drug delivery. *Front Neurol Neurosci* 36: 106-115.
- Chauhan NB (2002) Trafficking of intracerebroventricularly injected antisense oligonucleotides in the mouse brain. *Antisense Nucleic Acid Drug Dev* 12: 353-357.
- Westphal M, Ram Z, Riddle V, Hilt D, Bortey E (2006) Gliadel wafer in initial surgery for malignant glioma: long-term follow-up of a multicenter controlled trial. *Acta Neurochir* 148: 269-275.
- Lossinsky AS, Vorbrod AW, Wisniewski HM (1995) Scanning and transmission electron microscopic studies of microvascular pathology in the osmotically impaired blood-brain barrier. *J Neurocytol* 24: 795-806.
- Salahuddin TS, Johansson BB, Kalimo H, Olsson Y (1988) Structural changes in the rat brain after carotid infusions of hyperosmolar solutions. An electron microscopic study. *Acta Neuropathol* 77: 5-13.
- Doolittle ND, Petrillo A, Bell S, Cummings P, Eriksen S (1998) Blood-brain barrier disruption for the treatment of malignant brain tumors: The National Program. *J Neurosci Nurs* 30: 81-90.
- Jain KK (2012) Nanobiotechnology-based strategies for crossing the blood-brain barrier. *Nanomedicine (London)* 7: 1225-1233.
- Schlegel U, Pels H, Glasmacher A, Kleinschmidt R, Schmidt-Wolf I, et al. (2001) Combined systemic and intraventricular chemotherapy in primary CNS lymphoma: a pilot study. *J Neurol Neurosurg Psychiatry* 71: 118-122.
- Wohlfart S, Gelperina S, Kreuter J (2012) Transport of drugs across the blood-brain barrier by nanoparticles. *J Control Release* 161: 264-273.
- Fung LK, Shin M, Tyler B, Brem H, Saltzman WM (1996) Chemotherapeutic drugs released from polymers: distribution of 1,3-bis(2-chloroethyl)-1-nitrosourea in the rat brain. *Pharm Res* 13: 671-682.
- Blasberg RG, Patlak C, Fenstermacher JD (1975) Intrathecal chemotherapy: brain tissue profiles after ventriculocisternal perfusion. *J Pharmacol Exp Ther* 195: 73-83.
- Kreuter J, Alyautdin RN, Kharkevich DA, Ivanov AA (1995) Passage of peptides through the blood-brain barrier with colloidal polymer particles (nanoparticles). *Brain Res* 674: 171-174.
- Pardridge WM (2002) Drug and gene targeting to the brain with molecular Trojan horses. *Nat Rev Drug Discov* 1: 131-139.
- Re F, Gregori M, Masserini M (2012) Nanotechnology for neurodegenerative disorders. *Nanomedicine* S51-S58.
- Gaillard PJ, Visser CC, de Boer AG (2005) Targeted delivery across the blood-brain barrier. *Expert Opin Drug Deliv* 2: 299-309.
- Sahni JK, Doggui S, Ali J, Baboota S, Dao L, et al. (2011) Neurotherapeutic applications of Nanoparticles in Alzheimer's disease. *J Control Release* 152: 208-231
- Kreuter J (2001) Nanoparticulate systems for brain delivery of drugs. *Adv Drug Deliv Rev* 47: 65-81.
- Kreuter J (2014) Drug delivery to the central nervous system by polymeric nanoparticles: What do we know? *Adv Drug Deliv Rev* 71: 2-14.
- Zensi A, Begley D, Pontikis C, Legros C, Mihoreanu L, et al. (2009) Albumin nanoparticles targeted with Apo E enter the CNS by transcytosis and are delivered to neurones. *J Control Release* 137: 78-86.
- Wagner S, Zensi A, Wien SL, Tschickardt SE, Maier W, et al. (2012) Uptake mechanism of ApoE-modified nanoparticles on brain capillary endothelial cells as a blood-brain barrier model. *PLoS One* 7: e32568.
- Kreuter J, Hekmatara T, Dreis S, Vogel T, Gelperina S, et al. (2007) Covalent attachment of apolipoprotein A-I and apolipoprotein B-100 to albumin nanoparticles enables drug transport into the brain. *J Control Release* 118: 54-58.
- Kreuter J, Shamenkov D, Petrov V, Ramge P, Cychutek K, et al. (2002) Apolipoprotein-mediated transport of nanoparticle-bound drugs across the blood-brain barrier. *J Drug Target* 10: 317-325.
- Wagner S, Kufleitner J, Zensi A, Dadparvar M, Wien S, et al. (2010) Nanoparticulate transport of oximes over an *in vitro* blood-brain barrier model. *PLoS One* 5: e14213.
- Kulkarni RK, Pani KC, Neuman C, Leonard F (1966) Polylactic acid for surgical implants. *Arch Surg* 93: 839-843.
- Parepally JMR (2005) Factors limiting nonsteroidal anti-inflammatory drug uptake and distribution in central nervous system, Dissertation. Texas Tech University Health Sciences Center.
- Mannila A, Rautio J, Lehtonen M, Järvinen T, Savolainen J (2005) Inefficient central nervous system delivery limits the use of ibuprofen in neurodegenerative diseases. *Eur J Pharm Sci* 24: 101-105.
- Bannwarth B, Lapicque F, Pehourcq F, Gillet P, Schaeverbeke T, et al. (1995) Stereoselective disposition of ibuprofen enantiomers in human cerebrospinal fluid. *Br J Clin Pharmacol* 40: 266-269.

Citation: Stab J, Zlatev I, Raudszus B, Meister S, Pietrzik CU, et al. (2016) Flurbiprofen-loaded Nanoparticles Can Cross a Primary Porcine *In vitro* Blood-brain Barrier Model to Reduce Amyloid- β 42 Burden. J Nanomedicine Biotherapeutic Discov 6: 140. doi:[10.4172/2155-983X.1000140](https://doi.org/10.4172/2155-983X.1000140)

-
47. Matoga M, Péhourcq F, Lagrange F, Tramu G, Bannwarth B (1999) Influence of molecular lipophilicity on the diffusion of arylpropionate non-steroidal anti-inflammatory drugs into the cerebrospinal fluid. *Arzneimittelforschung* 49: 477-482.